CHEMISTRY OF MATERIALS

Communication

pubs.acs.org/cm

On the Mechanism of MOF-5 Formation under Cathodic Bias

Minyuan Li and Mircea Dincă*

Department of Chemistry, Massachusetts Institute of Technology, Cambridge, Massachusetts 02139, United States

Supporting Information

The considerable interest in the chemistry and applications of metal−organic frameworks (MOFs) has led to significant synthetic advances in this area, yet the details of the self-assembly process that give rise to these materials are still unclear. This is curious, but not unexpected: the crystallization of MOFs is difficult to study because their nucleation typically requires unpredictable induction periods that can vary from minutes to days, depending on the medium and metal−ligand pair, and is usually followed by rapid growth. Mechanistic studies are further complicated by the fact that many polymorphic structures are accessible from a single metal−ligand pair, although remarkable selectivity for a single crystalline phase is often observed under a given narrow set of conditions. This is evident in the rich literature on optimizing the synthesis of $Zn_4O(BDC)_3$ (MOF-5; BDC = 1,4-benzenedicarboxylate), one of the most iconic materials in the field, where precise control of water content, temperature, concentration, and pH are necessary to selectively form the $Zn_4O(O_2C-)_6$ secondary building units.[1−6]

Because electrochemistry confers highly reproducible reaction environments addressable by several variables that can be changed independently, it serves as a unique platform for fabricating integrated thin films,[7−14] and for studying the electrochemical growth of MOFs. As a widely recognized model system, we were particularly interested in the details of MOF-5 formation and its relation to other phases made from Zn^{2+} and BDC^{2-} ions.[8,15,16] For instance, we previously reported that MOF-5 can be deposited selectively at room temperature in 15 min on FTO electrodes under cathodic bias.[8] More recently, we have also shown that modulating the applied potential during electrolysis allowed access to heterobilayer structures of two Zn-BDC phases with high selectivity,[17] presumably by regulating the pH gradient near the electrode surface. Although electrochemical deposition allows the formation of complex heterostructures with high selectivity, finding the optimal conditions for depositing a given phase required significant empirical screening. Surmising that a deeper understanding of the mechanism of cathodic electrodeposition in the Zn-BDC system would facilitate the application of this method to other metal−ligand systems, we present here a more in-depth study aimed at elucidating the role of water and the supporting anions in the crystallization process and phase selection.

Our initial hypothesis was that hydroxide generation in the original MOF-5 electrochemical growth medium, which contained nitrate, water, and 1,4-benzenedicarboxylic acid, occurred by aqueous reduction of nitrate (eq 1). However, in principle, nitrate reduction does not require water. An electrochemical half-reaction can be written with 1,4-benzenedicarboxylic acid as the proton source (eq 2). In other words, electrodeposition should also occur from an initially anhydrous medium, in the absence of added water. Furthermore, in aqueous systems, water itself may function as a viable hydroxide source (eq 3), potentially obviating the need for nitrate. Thus, if eqs 2 and 3 become operative in the absence of water and nitrate, respectively, the role of these reagents in the electrochemical growth of MOF-5 could be systematically studied.

Although water reduction could produce hydroxide (eq 3), when the zinc source was switched from $Zn(NO_3)_2{\cdot}4.2H_2O$ to $Zn(ClO_4)_2{\cdot}6H_2O$ while holding all other experimental parameters constant, no MOFs were deposited (Figure S2 in the Supporting Information). This suggested that (1) nitrate was essential for electrochemical deposition, and (2) as a sole probase, water had a nearly negligible effect toward crystallization of MOF-5.

$$NO_3^- + H_2O + 2e^- \rightarrow NO_2^- + 2OH^- \quad (1)$$

$$NO_3^- + H_2BDC + 2e^- \rightarrow NO_2^- + H_2O + BDC^{2-} \quad (2)$$

$$H_2O + e^- \rightarrow \frac{1}{2}H_2 + OH^- \quad (3)$$

To investigate whether water had a role in nitrate reduction, we prepared an anhydrous solution of $Zn(NO_3)_2$ and tetra-*n*-butylammonium hexafluorophosphate ($TBAPF_6$) in *N*,*N*-dimethylformamide (DMF, see Experimental Details in the Supporting Information).[3] The use of this anhydrous electrodeposition medium enabled a series of experiments where the water content was systematically varied by combining different fractions of anhydrous $Zn(NO_3)_2$ and hydrated $Zn(NO_3)_2{\cdot}5H_2O$. As shown in Figure 1, electrolysis at −1.50 V in any of these solutions led to the electrodeposition of both MOF-5 and $Zn_3(BDC)_3(H_2O)_2{\cdot}4DMF$ regardless of the hydration level. Although the proportion of MOF-5 within this mixture increased with the water content, powder X-ray diffraction revealed reflections corresponding to MOF-5 even in the initially strictly anhydrous medium. Thus, in the absence of water, nitrate reduction is still operative, likely through eq 2. In other words, the electrodeposition of MOF-5 does not require water initially. We note, however, that if eq 2 is indeed responsible for nitrate reduction, water would be generated during electrolysis, such that even the initially anhydrous medium would become hydrated, possibly allowing both eqs 1 and 3 to take place under sustained cathodic bias. As established above, the in situ generation of water could further

Received: March 9, 2015
Revised: April 8, 2015
Published: April 21, 2015

DOI: 10.1021/acs.chemmater.5b00899
Chem. Mater. 2015, 27, 3203−3206

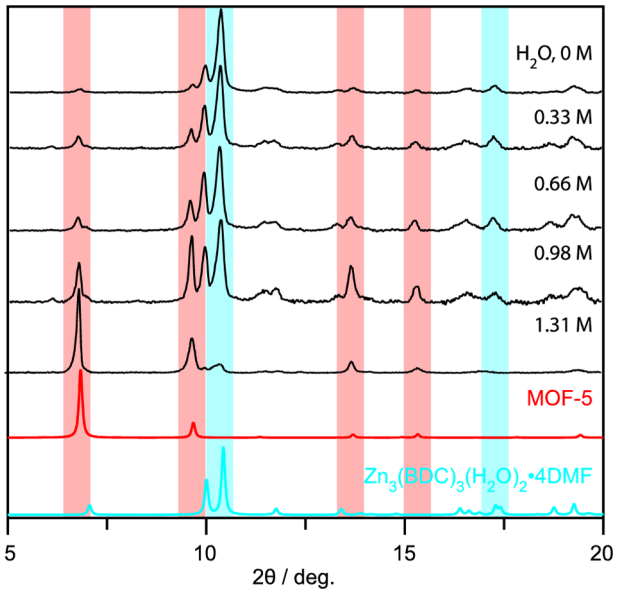

Figure 1. Normalized PXRD patterns of samples that were deposited on FTO at −1.50 V for 15 min at reagent concentrations of $[Zn(NO_3)_2]$ = 150 mM and $[H_2BDC]$ = 50 mM. The water content of the deposition baths was varied by combining different ratios of an anhydrous metathesized $Zn(NO_3)_2$ solution in DMF-anh (0 M H_2O) and a hydrated $Zn(NO_3)_2{\cdot}5H_2O$ solution in DMF-hyd (1.31 M H_2O). The patterns of MOF-5 and $Zn_3(BDC)_3(H_2O)_2{\cdot}4DMF$ were simulated.[25,26] See Figure S3 in the Supporting Information.

change the composition of the electrodeposited MOF film, biasing it toward the formation of MOF-5 at the expense of $Zn_3(BDC)_3(H_2O)_2{\cdot}4DMF$.

Another set of experiments aimed at establishing the role of nitrate and water in the electrodeposition process focused on systematically varying the Zn^{2+} source by choosing different supporting anions and by varying the hydration level of the deposition bath. $Zn(ClO_4)_2{\cdot}6H_2O$, $ZnCl_2$ (anh.), and $Zn(CF_3SO_3)_2$ (anh.) were chosen as the sources of Zn^{2+} ions. These Zn^{2+} precursors were dissolved together with H_2BDC and $NaNO_3$ in either anhydrous DMF (DMF-anh) or hydrated DMF (DMF-hyd) deposition baths. A total of six deposition baths were prepared, two for each Zn^{2+} starting material, with varying levels of hydration (see Table 1). For example, dissolving anhydrous $ZnCl_2$, $NaNO_3$, and H_2BDC in DMF-anh yielded a rigorously anhydrous medium that was similar to that described above for the anhydrous $Zn(NO_3)_2$ experiment, except for the presence of chloride anions. In contrast, dissolving $Zn(ClO_4)_2{\cdot}6H_2O$, $NaNO_3$, and H_2BDC in

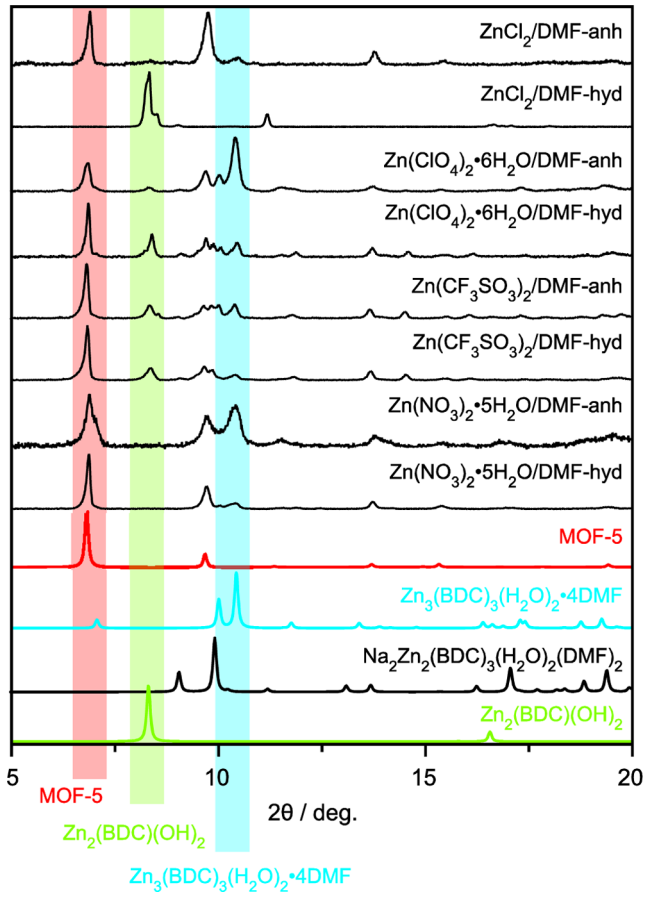

Figure 2. Normalized PXRD patterns of samples that were deposited under −1.50 V on FTO substrates in DMF-anh and DMF-hyd for 15 min with reagent concentrations of $[ZnCl_2]$, $[Zn(ClO_4)_2{\cdot}6H_2O]$, $[Zn(CF_3SO_3)_2]$ = 150 mM, $[NaNO_3]$ = 300 mM, and $[H_2BDC]$ = 50 mM. The PXRD patterns of MOF-5, $Zn_3(BDC)_3(H_2O)_2{\cdot}4DMF$, and $Na_2Zn_2(BDC)_3(H_2O)_2(DMF)_2$ were simulated.[25−27] The PXRD pattern of $Zn_2(BDC)(OH)_2$ was simulated with a preferential orientation along (001) with a March-Dollase parameter of 0.5, corresponding to the extended Zn-μ_3−OH sheets bridged by BDC^{2-}.[22,23] See Figures S4 and S5 in the Supporting Information.

DMF-hyd yielded a solution with a hydration level similar to that described in our original report, which used $Zn(NO_3)_2{\cdot}4.2H_2O$ in DMF-hyd.[8] As shown in Figure 2, the deposits obtained after 15 min from these six solutions under a cathodic bias of −1.50 V were generally similar, with MOF-5 featuring prominently in five of the six deposition baths. In these five cases, the nitrate anions from the $NaNO_3$ electrolyte promoted

Table 1. Deposition Bath Parameters[a] and Solid Species Identified by PXRD

Zn source	DMF solvent	$[H_2O]$ (mM)	observed crystalline phases	$[Na^+]$ = $[X^-]$ (mM)
$ZnCl_2$	anh	0	MOF-5, $Zn_3(BDC)_3(H_2O)_2{\cdot}4DMF$	$[Cl^-]$ = 300
$ZnCl_2$	hyd	560	$Zn_2(BDC)(OH)_2$, $Zn_5(OH)_8(H_2O)_2{\cdot}(NO_3)_2$, $Zn_5(OH)_8(Cl)_2{\cdot}(H_2O)_2$	$[Cl^-]$ = 300
$Zn(CF_3SO_3)_2$	anh	0	MOF-5, $Zn_3(BDC)_3(H_2O)_2{\cdot}4DMF$, $Zn_2(BDC)(OH)_2$, $Na_2Zn_2(BDC)_3(H_2O)_2(DMF)_2$	$[CF_3SO_3^-]$ = 300
$Zn(CF_3SO_3)_2$	hyd	560	MOF-5, $Zn_3(BDC)_3(H_2O)_2{\cdot}4DMF$, $Zn_2(BDC)(OH)_2$, $Na_2Zn_2(BDC)_3(H_2O)_2(DMF)_2$	$[CF_3SO_3^-]$ = 300
$Zn(ClO_4)_2{\cdot}6H_2O$	anh	900	MOF-5, $Zn_3(BDC)_3(H_2O)_2{\cdot}4DMF$, $Zn_2(BDC)(OH)_2$, $Na_2Zn_2(BDC)_3(H_2O)_2(DMF)_2$	$[ClO_4^-]$ = 300
$Zn(ClO_4)_2{\cdot}6H_2O$	hyd	1460	MOF-5, $Zn_3(BDC)_3(H_2O)_2{\cdot}4DMF$, $Zn_2(BDC)(OH)_2$, $Na_2Zn_2(BDC)_3(H_2O)_2(DMF)_2$	$[ClO_4^-]$ = 300
$Zn(NO_3)_2{\cdot}5H_2O$	anh	750	MOF-5, $Zn_3(BDC)_3(H_2O)_2{\cdot}4DMF$	0
$Zn(NO_3)_2{\cdot}5H_2O$	hyd	1310	MOF-5, $Zn_3(BDC)_3(H_2O)_2{\cdot}4DMF$	0
$Zn(NO_3)_2$ (anh)	anh	0	MOF-5, $Zn_3(BDC)_3(H_2O)_2{\cdot}4DMF$	0

[a] $[Zn^{2+}]$ = 150 mM, $[NO_3^-]$ = 300 mM.

DOI: 10.1021/acs.chemmater.5b00899
Chem. Mater. 2015, 27, 3203−3206

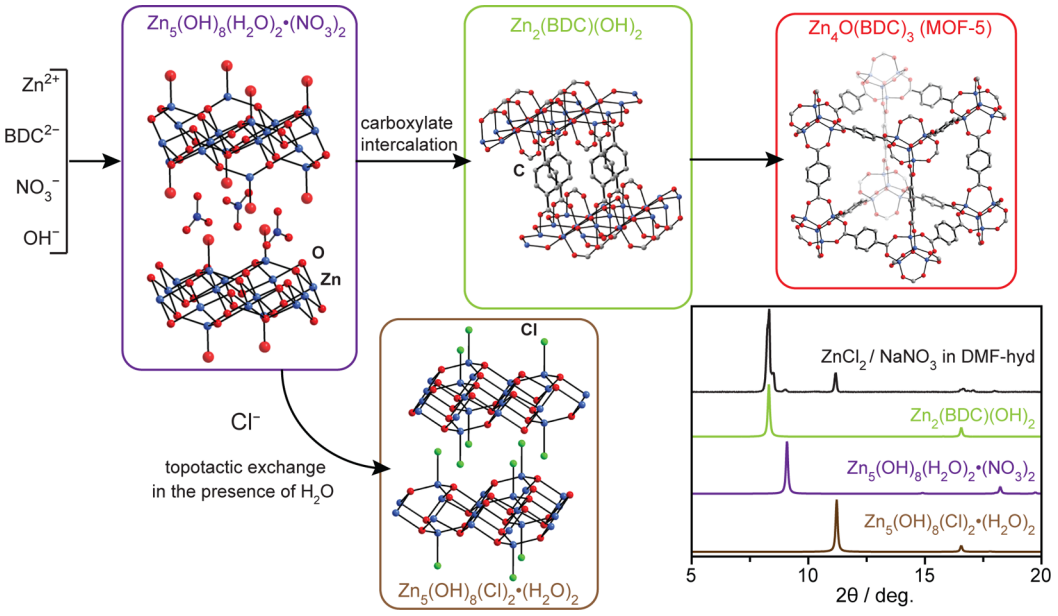

Figure 3. Proposed transformation scheme to account for the different crystalline phases observed during the electrochemically induced growth of MOF-5. The inset shows the experimental PXRD pattern of a sample deposited at −1.50 V on FTO in DMF-hyd for 15 min with reagent concentrations of [$ZnCl_2$] = 150 mM, [$NaNO_3$] = 300 mM, and [H_2BDC] = 50 mM. The PXRD patterns of $Zn_5(OH)_8(H_2O)_2{\cdot}(NO_3)_2$[20] and $Zn_5(OH)_8(Cl)_2{\cdot}(H_2O)_2$[28] were simulated. The PXRD pattern of $Zn_2(BDC)(OH)_2$ was simulated with a preferential orientation along (001).[22,23]

the fast and robust formation of MOF-5 regardless of the hydration level. However, MOF-5 was strikingly absent when $ZnCl_2$ was used as a precursor in DMF-hyd, even though MOF-5 was deposited from DMF-anh and $ZnCl_2$. Instead of MOF-5, electrolysis from $ZnCl_2$ in DMF-hyd led to the formation of $Zn_2(BDC)(OH)_2$ along with a layered zinc hydroxychloride, $Zn_5(OH)_8(Cl)_2{\cdot}(H_2O)_2$ (Figure 3). Thus, in hydrated solutions, chloride anions completely inhibited the formation of MOF-5.

The ability of Cl^- to inhibit the formation of MOF-5 has been noted previously: published solvothermal routes to MOF-5 almost invariably use $Zn(NO_3)_2$, and one report states that heating $ZnCl_2$ and H_2BDC in *N*,*N*-diethylformamide at 110 °C for 48 h produced no crystalline precipitates.[4] What is more puzzling is why the layered hydroxychloride phase, containing Zn-μ_3−OH sheets, is deposited from DMF-hyd, but not from DMF-anh, where hydroxide anions are still available through NO_3^- reduction. One possibility is that the formation of this hydroxychloride requires both water and hydroxide. Intriguingly, $Zn_5(OH)_8(Cl)_2{\cdot}(H_2O)_2$ is also known to form rapidly when a related layered hydroxynitrate, $Zn_5(OH)_8(H_2O)_2{\cdot}(NO_3)_2$, is topotactically intercalated with Cl^-.[18] Thus, it is possible that $Zn_5(OH)_8(Cl)_2{\cdot}(H_2O)_2$ evolves from $Zn_5(OH)_8(H_2O)_2{\cdot}(NO_3)_2$. Although the latter is not observed in the absence of Cl^-, it is indeed accessible from aqueous solutions of $Zn(NO_3)_2$,[19−21] under conditions that mimic those created under cathodic bias in our deposition medium. Most importantly, these layered hydroxide phases may serve as precursors to the formation of $Zn_2(BDC)(OH)_2$, a metastable phase with zinc hydroxide layers bridged by BDC^{2-},[22,23] which we observed in all depositions that used non-nitrate Zn^{2+} precursors (Figure 2).

These observations lend support to the idea that MOF-5 growth is preceded by the formation of metastable layered zinc hydroxide phases (see Figure 3).[6,24] Thus, the fact that MOF-5 formation is vastly accelerated by nitrate anions in both solvothermal and electrochemical routes may reflect the importance of these layered hydroxide phases, and especially of $Zn_5(OH)_8(H_2O)_2{\cdot}(NO_3)_2$, as intermediates (Figure S6 in the Supporting Information).[6,8,24] Furthermore, they highlight a potentially important structural role for nitrate in giving rise to these intermediate phases, a role that has not yet been recognized.

Evidence for the formation of the key intermediate, $Zn_5(OH)_8(H_2O)_2{\cdot}(NO_3)_2$, came from experiments that varied the postelectrolysis treatment of films deposited from $ZnCl_2$/$NaNO_3$. Thus, if freshly deposited films were immediately soaked in neat anhydrous DMF, thereby completely eliminating their continued exposure to water, only $Zn_5(OH)_8(H_2O)_2{\cdot}(NO_3)_2$ and $Zn_2(BDC)(OH)_2$ were observed, while $Zn_5(OH)_8(Cl)_2{\cdot}(H_2O)_2$ was absent (Figure 4). The same films showed weak, but discernible reflections corresponding to MOF-5 itself. If fresh deposits were instead soaked in DMF-hyd for 3 h, a solvent that more closely resembles our deposition media, strong reflections corresponding to $Zn_5(OH)_8(Cl)_2{\cdot}(H_2O)_2$ were observed, while reflections corresponding to $Zn_2(BDC)(OH)_2$ were weak, and those corresponding to other phases, including MOF-5, were absent. These experiments suggested that $Zn_5(OH)_8(Cl)_2{\cdot}(H_2O)_2$ is formed only when both chloride and water are present in abundance. The formation of this phase and/or the continued exposure to water, which is known to assist in the decomposition of MOF-5, may also contribute to the absence of reflection peaks for the latter when the films are left in a hydrated medium.

Taken together, the foregoing results highlight the essential role of nitrate in the formation of the $Zn_4O(O_2C-)_6$ secondary building units in MOF-5 on fluorine-doped tin oxides. Although water is not required initially, it is generated in situ during nitrate reduction in the presence of protons. Surprisingly, we also observed various Zn-μ_3−OH species in the presence of other counteranions, which may be relevant to the progression of crystalline phases proposed in the solvothermal process, most notably a transient layered $Zn_5(OH)_8(H_2O)_2{\cdot}(NO_3)_2$ phase. Nitrate anions therefore

DOI: 10.1021/acs.chemmater.5b00899
Chem. Mater. 2015, 27, 3203−3206

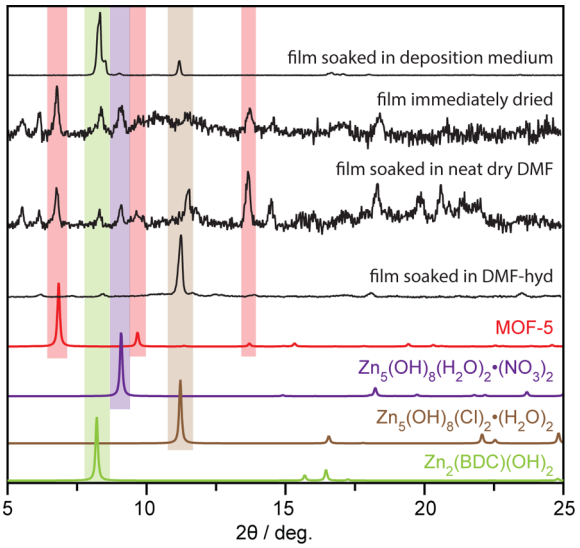

Figure 4. Normalized experimental PXRD patterns of samples deposited at −1.50 V on FTO in DMF-hyd for 15 min with reagent concentrations of [$ZnCl_2$] = 150 mM, [$NaNO_3$] = 300 mM, and [H_2BDC] = 50 mM. PXRD patterns of $Zn_5(OH)_8(H_2O)_2{\cdot}(NO_3)_2$[20] and $Zn_5(OH)_8(Cl)_2{\cdot}(H_2O)_2$[28] were simulated. The PXRD pattern of $Zn_2(BDC)(OH)_2$ was simulated with a preferential orientation along (001).[22,23]

play essential roles both chemically, initiating the formation of base and the electrochemical deposition, and structurally, with the formation of the layered phase.

■ ASSOCIATED CONTENT

Supporting Information

Additional experiment details, scanning electron micrographs, PXRD patterns. The Supporting Information is available free of charge on the ACS Publications website at DOI: 10.1021/acs.chemmater.5b00899.

■ AUTHOR INFORMATION

Corresponding Author

*E-mail: mdinca@mit.edu.

Notes

The authors declare no competing financial interest.

■ ACKNOWLEDGMENTS

This work was supported by the U.S. Department of Energy, Office of Science, Office of Basic Energy Sciences (Award DE-SC0006937). M.D. thanks 3M, the Sloan Foundation, and the Research Corporation for Science Advancement for non-tenured faculty funds. M.L. is partially supported by an NSF Graduate Research Fellowship (Grant 1122374). We thank K. Armburst for assistance with coulometry. Part of this work was performed at the Center for Nanoscale Systems (CNS) at Harvard University. CNS is a member of the National Nanotechnology Infrastructure Network, which is supported by the NSF under Award ECS-0335765.

■ REFERENCES

(1) Huang, L.; Wang, H.; Chen, J.; Wang, Z.; Sun, J.; Zhao, D.; Yan, Y. *Microporous Mesoporous Mater.* **2003**, *58* (2), 105−114.
(2) Kaye, S. S.; Dailly, A.; Yaghi, O. M.; Long, J. R. *J. Am. Chem. Soc.* **2007**, *129* (46), 14176−14177.
(3) Hausdorf, S.; Wagler, J.; Mossig, R.; Mertens, F. O. R. L. *J. Phys. Chem. A* **2008**, *112* (33), 7567−7576.
(4) Biemmi, E.; Christian, S.; Stock, N.; Bein, T. *Microporous Mesoporous Mater.* **2009**, *117* (1−2), 111−117.
(5) Kim, H.; Das, S.; Kim, M. G.; Dybtsev, D. N.; Kim, Y.; Kim, K. *Inorg. Chem.* **2011**, *50* (8), 3691−3696.
(6) McKinstry, C.; Cussen, E. J.; Fletcher, A. J.; Patwardhan, S. V.; Sefcik, J. *Cryst. Growth Des.* **2013**, *13* (12), 5481−5486.
(7) Ameloot, R.; Stappers, L.; Fransaer, J.; Alaerts, L.; Sels, B. F.; De Vos, D. E. *Chem. Mater.* **2009**, *21* (13), 2580−2582.
(8) Li, M.; Dincă, M. *J. Am. Chem. Soc.* **2011**, *133* (33), 12926−12929.
(9) Joaristi, A. M.; Juan-Alcaniz, J.; Serra-Crespo, P.; Kapteijn, F.; Gascon, J. *Cryst. Growth Des.* **2012**, *12* (7), 3489−3498.
(10) Campagnol, N. N.; Van Assche, T.; Boudewijns, T.; Denayer, J.; Binnemans, K.; De Vos, D.; Fransaer, J. *J. Mater. Chem. A* **2013**, *1* (19), 5827−5830.
(11) Stassen, I.; Styles, M.; Van Assche, T.; Campagnol, N.; Fransaer, J.; Denayer, J.; Tan, J.-C.; Falcaro, P.; De Vos, D.; Ameloot, R. *Chem. Mater.* **2015**, *27* (5), 1801−1807.
(12) Yadnum, S.; Roche, J.; Lebraud, E.; Négrier, P.; Garrigue, P.; Bradshaw, D.; Warakulwit, C.; Limtrakul, J.; Kuhn, A. *Angew. Chem., Int. Ed.* **2014**, *53* (15), 4001−4005.
(13) Hod, I.; Bury, W.; Karlin, D. M.; Deria, P.; Kung, C. W.; Katz, M. J.; So, M.; Klahr, B.; Jin, D.; Chung, Y. W.; Odom, T. W.; Farha, O. K.; Hupp, J. T. *Adv. Mater.* **2014**, *26* (36), 6295−6300.
(14) Campagnol, N.; Souza, E. R.; De Vos, D. E.; Binnemans, K.; Fransaer, J. *Chem. Commun.* **2014**, *50*, 12545−12547.
(15) Ameloot, R.; Gobechiya, E.; Uji-i, H.; Martens, J. A.; Hofkens, J.; Alaerts, L.; Sels, B. F.; De Vos, D. E. *Adv. Mater.* **2010**, *22* (24), 2685−2688.
(16) Liu, H.; Wang, H.; Chu, T.; Yu, M.; Yang, Y. *J. Mater. Chem. C* **2014**, *2* (41), 8683−8690.
(17) Li, M.; Dincă, M. *Chem. Sci.* **2014**, *5* (1), 107−111.
(18) Stählin, W.; Oswald, H. R. *J. Solid State Chem.* **1971**, *3* (2), 256−264.
(19) Bøjesen, E. D.; Jensen, K. M. Ø.; Tyrsted, C.; Lock, N.; Christensen, M.; Iversen, B. B. *Cryst. Growth Des.* **2014**, *14* (6), 2803−2810.
(20) Stählin, W.; Oswald, H. R. *Acta Crystallogr., Sect. B* **1970**, *26* (6), 860−863.
(21) Li, P.; Xu, Z. P.; Hampton, M. A.; Vu, D. T.; Huang, L.; Rudolph, V.; Nguyen, A. V. *J. Phys. Chem. C* **2012**, *116* (18), 10325−10332.
(22) Carton, A.; Mesbah, A.; Aranda, L.; Rabu, P.; François, M. *Solid State Sci.* **2009**, *11* (4), 818−823.
(23) Carton, A.; Abdelouhab, S.; Renaudin, G.; Rabu, P.; François, M. *Solid State Sci.* **2006**, *8* (8), 958−963.
(24) Zheng, C.; Greer, H. F.; Chiang, C.-Y.; Zhou, W. *CrystEngComm* **2014**, *16* (6), 1064.
(25) Li, H.; Eddaoudi, M.; O'Keeffe, M.; Yaghi, O. M. *Nature* **1999**, *402* (6759), 276−279.
(26) Edgar, M.; Mitchell, R.; Slawin, a M.; Lightfoot, P.; Wright, P. A. *Chem.—Eur. J.* **2001**, *7* (23), 5168−5175.
(27) Yang, S.-Y.; Sun, Z.-G.; Long, L.-S.; Huang, R.-B.; Zheng, L.-S. *Main Group Met. Chem.* **2002**, *25* (9), 699−700.
(28) Hawthorne, F. C.; Sokolova, E. *Can. Miner.* **2002**, *40* (3), 939−946.

DOI: 10.1021/acs.chemmater.5b00899
Chem. Mater. 2015, 27, 3203−3206